A constitutive model for sands under cyclic shear stresses

Un modèle constitutif pour sables sous contraintes cycliques

H. MATSUOKA, Associate Professor, Nagoya Institute of Technology, Nagoya, Japan
H. KOYAMA, Engineer, Ohbayashi-gumi Ltd., Tokyo, Japan

SYNOPSIS A constitutive model for sands is proposed supposing the superposition of strain increments caused by three imaginary two-dimensional slip planes under the respective two principal stresses and considering the mechanism of fabric change due to cyclic shear stresses. The results of drained true triaxial tests along rotational stress paths on the octahedral plane, the undrained effective stress paths and the liquefaction resistances under cyclic triaxial compression and extension conditions are analyzed by the proposed model.

INTRODUCTION

Recently, rotational stress paths on the octahedral plane and on the simple shear plane have attracted attention in connection with the ground motions during earthquakes. A constitutive model for sands is presented on the basis of the theory of "compounded mobilized planes", which suppose three two-dimensional slip planes between the respective two principal stress directions, and the consideration of the mechanism of fabric change under cyclic loading. It can explain well the results of various kinds of true triaxial tests along not only radial stress paths but also rotational stress paths on the octahedral plane. Adding the strains due to consolidation to the above-mentioned model and considering the undrained condition of no volumetric strain increments, undrained effective stress paths under cyclic loading are analyzed. From the analytical results, the relationship between the cyclic stress ratio and the number of cycles to produce the initial liquefaction is obtained, and it agrees well with the experimental results by undrained cyclic triaxial compression and extension tests on sand.

A CONSTITUTIVE MODEL BASED ON "MOBILIZED PLANES"

The proposed model is formulated on the basis of the following postulates(Matsuoka, 1974b,1982): 1) Each of three principal strain increments $d\varepsilon_1$, $d\varepsilon_2$ and $d\varepsilon_3$ is expressed as the sum of the two components produced by two imaginary two-dimensional slip planes between the corresponding two principal stress directions. 2) The yield condition is determined independently by each of principal stress ratios(σ_1/σ_2, σ_2/σ_3 and σ_1/σ_3) between the respective two principal stress directions. 3) As the above-mentioned three two-dimensional slip planes, the "mobilized planes" on which shear-normal stress ratios are maximized between the respective two principal stress directions are selected(see Figs.1 and 2), and the two-dimensional stress-strain relationships on the potential slip plane, which have been derived from the microscopic shear mechanism, hold on the "mobilized plane"(Matsuoka, 1974a; Matsuoka and Geka, 1983).

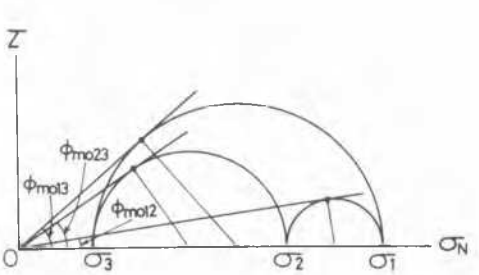

Fig.1 Stress States on Three Mobilized Planes on Which Shear-normal Stress Ratios are Maximized under Respective Two Principal Stresses

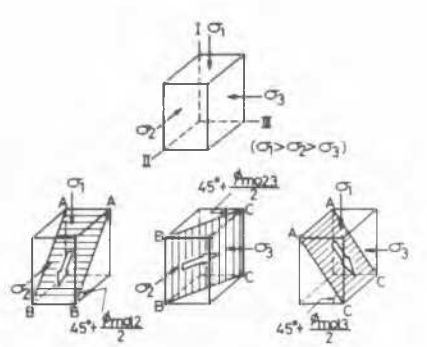

Fig.2 Three Two-dimensional Mobilized Planes under Three Principal Stresses Which are Called "Compounded Mobilized Planes"

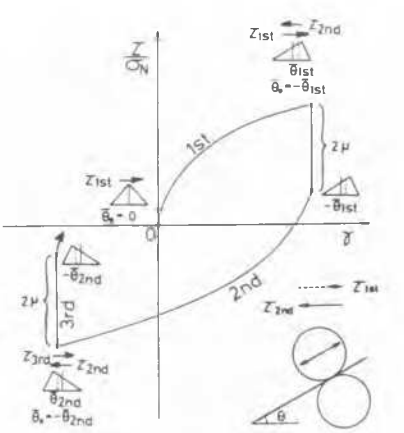

Fig.3 Variation in the Triangular Frequency Distribution of Interparticle Contact Angles θ Caused by Cyclic Stresses

Based on the aforementioned postulates 1) and 3), the principal strain increments($d\varepsilon_1$, $d\varepsilon_2$ and $d\varepsilon_3$) under three principal stresses are given by the following equations(Matsuoka, 1974b,1982).

$$d\varepsilon_1 = f'(\frac{\sigma_1}{\sigma_3})\cdot dX_{13} + f'(\frac{\sigma_1}{\sigma_2})\cdot dX_{12} \quad (1)$$

$$d\varepsilon_2 = f'(\frac{\sigma_2}{\sigma_3})\cdot dX_{23} + g'(\frac{\sigma_1}{\sigma_2})\cdot dX_{12} \quad (2)$$

$$d\varepsilon_3 = g'(\frac{\sigma_1}{\sigma_3})\cdot dX_{13} + g'(\frac{\sigma_2}{\sigma_3})\cdot dX_{23} \quad (3)$$

in which

$$f'(\frac{\sigma_i}{\sigma_j}) = \frac{\gamma_{oij}}{\mu'_{ij}-\mu}\cdot(\frac{\mu-X_{ij}}{\lambda} + \frac{1}{2}\sqrt{\frac{\sigma_i}{\sigma_j}})\cdot\exp(\frac{X_{ij}-\mu}{\mu'_{ij}-\mu}) \quad (4)$$

$$g'(\frac{\sigma_i}{\sigma_j}) = \frac{\gamma_{oij}}{\mu'_{ij}-\mu}\cdot(\frac{\mu-X_{ij}}{\lambda} - \frac{1}{2}\sqrt{\frac{\sigma_j}{\sigma_i}})\cdot\exp(\frac{X_{ij}-\mu}{\mu'_{ij}-\mu}) \quad (5)$$

$$X_{ij} = \tan\phi_{moij} = (\sqrt{\sigma_i/\sigma_j} - \sqrt{\sigma_j/\sigma_i})/2 \qquad (i,j = 1, 2, 3;\ i<j) \quad (6)$$

In the above soil parameters (λ, μ, μ'_{ij} and γ_{oij}), λ and $\mu(=\tan\phi_\mu)$ are considered to be material constants, and μ'_{ij} and γ_{oij} are parameters to evaluate the fabric change as described later.

EVALUATION OF CYCLIC SHEAR STRESS HISTORY

Fig.3 shows the conceptional relationship between a stress-strain behaviour under cyclic loading and the variation in the triangular frequency distribution of interparticle contact angles θ along the mobilized plane. $\bar{\theta}$ is the average value of θ, and $\bar{\theta}_o$ is $\bar{\theta}$ at the beginning of shear. The following relation between τ/σ_N and $\bar{\theta}$ holds (Matsuoka, 1974a; Matsuoka and Geka, 1983).

$$\tau/\sigma_N = \lambda\cdot\bar{\theta} + \mu \quad (7)$$

As the particles are rearranged so as to resist the shear stress τ_{1st} under the 1st loading, the frequency distribution is one-sided to the right side of θ. If the particles are then subjected to τ_{2nd} in the reverse direction, they slide down easily and thus the stress-strain curve under the 2nd loading becomes gentle comparing with that under the 1st loading. It should be noted that $\bar{\theta}_o$ under the 2nd loading is considered to be $-\bar{\theta}_{1st}$ where $\bar{\theta}_{1st}$ is $\bar{\theta}$ at the end of the 1st loading(see Fig.3). It is assumed that when sheared in the reverse direction the distribution of contact angles is not changed and the strains are not caused in $\Delta(\tau/\sigma_N)=2\mu(=2\tan\phi_\mu)$ by the action of interparticle friction. $\bar{\theta}_o$ and $\bar{\theta}_f(=\bar{\theta}$ at failure) are reflected to soil parameters μ'_{ij} and γ_{oij} by the following equations(Matsuoka and Geka, 1983).

$$\mu'_{ij} - \mu = \kappa\cdot(\bar{\theta}_f - \bar{\theta}_o) \quad (8)$$

$$\gamma_{oij} = \gamma_{olst}\cdot\exp[\lambda(-\bar{\theta}_o)/\{\kappa(\bar{\theta}_f-\bar{\theta}_o)\}] \quad (9)$$

in which γ_{olst} is γ_{oij} under the 1st loading and κ is a parameter given by the following equation.

$$\kappa = (\mu'_{1st} - \mu)/\bar{\theta}_f \quad (10)$$

in which μ'_{1st} is μ'_{ij} under the 1st loading. If parameters under the 1st loading(λ, μ, μ'_{1st} and γ_{olst}) and shear strength are obtained from the conventional monotonic loading test, parameters under reverse shear stresses(μ'_{ij} and γ_{oij}) can be estimated one after another by Eqs.(7)-(10).

TRUE TRIAXIAL TESTS ALONG ROTATIONAL STRESS PATHS

The specimens(96mm×96mm×111mm, void ratio after isotropic compression $e_o\fallingdotseq0.66$) were made by

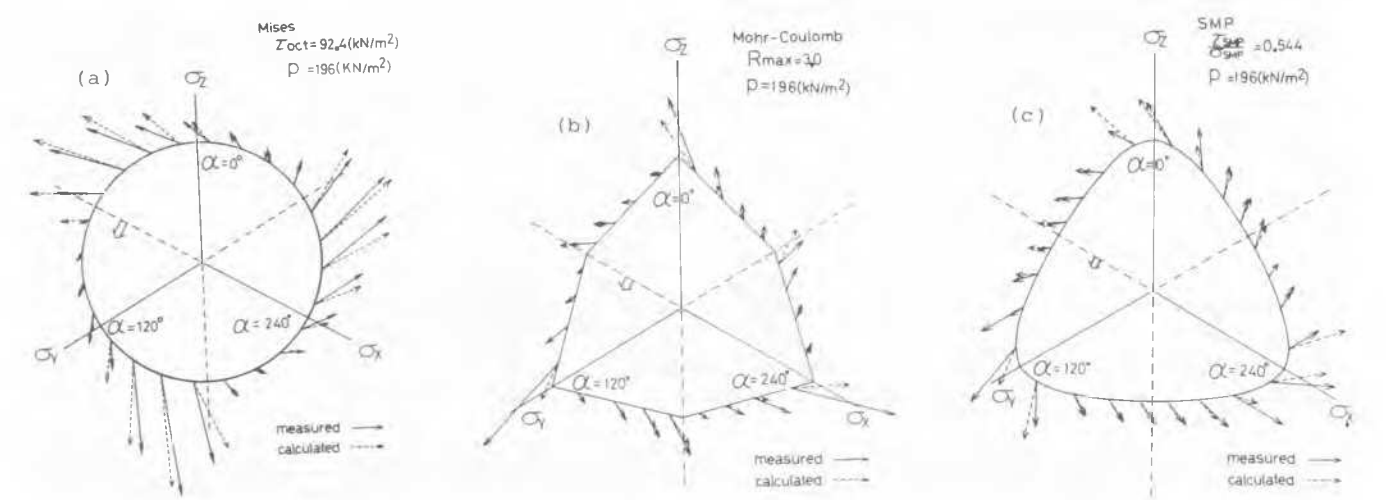

Fig.4 Comparison of Measured Values with Calculated Values of Octahedral Shear Strain Increments under Three Kinds of Rotational Stress Paths((a)Mises, (b)Mohr-Coulomb and (c)Matsuoka-Nakai Criteria)

pouring saturated Toyoura sand(D_{50}=0.2mm, U_c=1.3, G_s=2.65, e_{max}=0.95 and e_{min}=0.58) with a spoon into the rectangular rubber bag in the true triaxial apparatus, and by plunging an iron rod (φ10mm) with eddy motion into the sand layer to make an isotropic sample. Three principal stresses were independently applied to the specimen by three pairs of rigid loading plates(Matsuoka, 1982). The stress paths used are such rotational paths on the octahedral plane(effective mean principal stress p=196 kN/m^2) as a circle (Mises criterion), an irregular hexagon(Mohr-Coulomb criterion) and a "rounded triangle" circumscribed with the Mohr-Coulomb criterion(Matsuoka-Nakai criterion, 1974). The Matsuoka-Nakai criterion has been proposed on the assumption that soils fail when the shear-normal stress ratio on the "spatial mobilized plane (SMP)", which is a plane ABC with three mobilized planes AB, BC and AC in Fig.2 as the three sides, reaches a limiting value. It is expressed as follows(Matsuoka and Nakai, 1974,1977).

$$J_1 \cdot J_2 / J_3 = \text{const.} \qquad (11)$$

or

$$\tan^2\phi_{mo12} + \tan^2\phi_{mo23} + \tan^2\phi_{mo13} = \text{const.} \qquad (12)$$

in which J_1, J_2 and J_3 are the first, second and third effective stress invariants.

Figs.4(a) to (c) show the comparison of the measured values(solid arrows) with the calculated values by the proposed model(dotted arrows) of the octahedral shear strain increments $d\gamma_{oct}$ under the three kinds of rotational stress paths. These three kinds of tests are all carried out by shearing up to the fixed major and minor principal stress ratio R(R=3 or 4) under the triaxial extension condition and then turning along the rotational stress paths to the direction of the white arrows shown in Fig.4. The magnitude of the solid and dotted arrows in Fig.4 denotes the ratio($d\gamma_{oct}/d\alpha$) where α is the angle from the σ_z direction. It should be noted in Fig.4(a) that $d\gamma_{oct}$ becomes large in the ranges(α=0°~60°, 120°~180°, 240°~300°) where R increases and it becomes small in the ranges (α=60°~120°, 180°~240°, 300°~360°) where R decreases. It is concluded from the experimental fact in Fig.4(a) that the Mises criterion is improper for the yield condition of sands. As seen from Figs.4(b) and (c), the plastic strains are also produced in the rotational stress paths along the Mohr-Coulomb criterion and the Matsuoka-Nakai criterion. Therefore, the Mohr-Coulomb criterion and the Matsuoka-Nakai criterion which are suitable for the failure criteria of soils are not proper for the yield condition in the strict sense. Considering the well agreement of the measured values with the calculated ones in Figs.4(a) to (c), it may be supposed that the proposed two-dimensional yield condition due to the increase in principal stress ratios σ_1/σ_2, σ_2/σ_3 and σ_1/σ_3 is fit for the nature of soils. Figs.5(a) to (c) show the comparison of the measured values(plots) with the calculated values of three principal strains(ε_Z, ε_Y and ε_X) and volumetric strain(ε_v) against α, when the stress state are rotated along the Mises, Mohr-Coulomb and Matsuoka-Nakai criteria shown in Fig.4. The soil parameters used for the calculation are as follows: λ=1.2, μ=0.20, μ'_{ist}=0.36, γ_{olst}=0.06%(at p=196kN/m^2) and the principal stress ratio at failure R_f=4.6(ϕ_d=40°), which can be determined by a triaxial compression test(p=196kN/m^2) on the cylindrical Toyoura sand specimen.

ANALYSIS OF LIQUEFACTION RESISTANCES

Adding the strains due to consolidation to the strains described by Eqs.(1)-(3), and considering the undrained condition of no volumetric strain increments($d\varepsilon_v$=0), the following equation is obtained when the effective mean principal stress p decreases($dp \leqq 0$).

$$\begin{aligned} d\varepsilon_v = {} & \{f'(\sigma_1/\sigma_3) + g'(\sigma_1/\sigma_3)\}\cdot dX_{13} \\ & + \{f'(\sigma_1/\sigma_2) + g'(\sigma_1/\sigma_2)\}\cdot dX_{12} \\ & + \{f'(\sigma_2/\sigma_3) + g'(\sigma_2/\sigma_3)\}\cdot dX_{23} \\ & + \{0.434C_s/(1+e_o)\}\cdot(dp/p) = 0 \end{aligned} \qquad (13)$$

The undrained effective stress paths can be calculated from Eq.(13). Fig.6 shows an analytical result of effective stress path in an

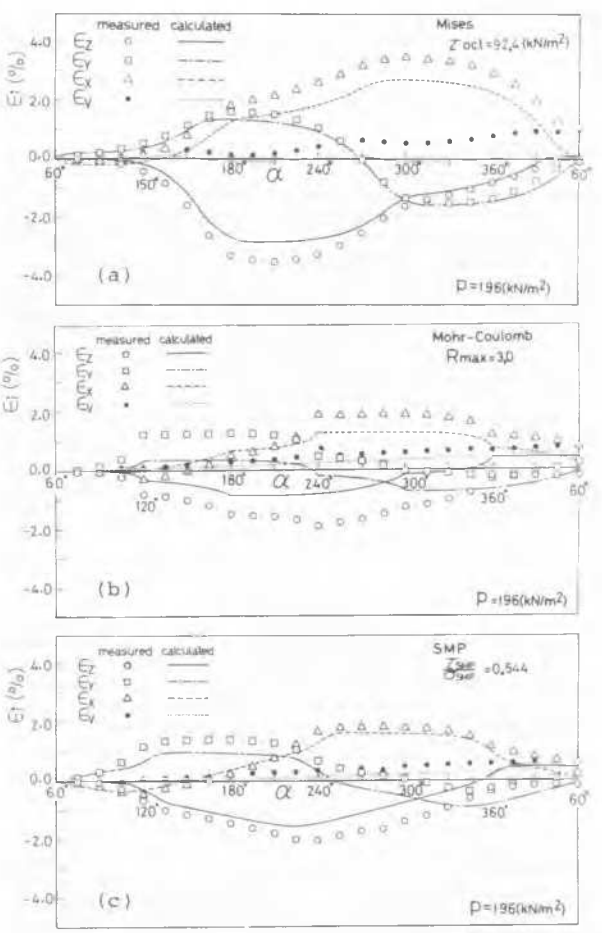

Fig.5 Comparison of Measured Values with Calculated Values of Three Principal Strains and Volumetric Strain against α When Rotated along (a)Mises, (b)Mohr-Coulomb and (c)Matsuoka-Nakai Criteria

undrained cyclic triaxial compression and extension test under the condition of maximum principal stress difference q=39.2kN/m^2 and initial effective mean principal stress p_o=98kN/m^2($q=\sigma_a-\sigma_r$, σ_a:axial principal stress, σ_r:radial principal stress). In this figure, η_f, η_m and η_μ represent the values of q/p at failure, at the "phase transformation"(Ishihara et al, 1975) and at $\tau/\sigma_N=\mu$ corresponding to the coefficient of interparticle friction respectively. Fig.7 represents the measured and calculated relationships between the cyclic stress ratio $q/2p_o$ and the number of cycles to produce the initial liquefaction. The measured values in this figure are obtained by Muramatsu(1981). The initial liquefaction is here defined as DA(double amplitude) axial strain=2%. γ_{olst}=0.04% corresponds nearly to the parameter for Toyoura sand of D_r=80%. It is seen from this figure that the analytical results explain well the measured values. The parameters used for the above analysis are γ_{olst}=0.04%(at p=98kN/m^2), $C_s/(1+e_o)$=0.578%, K_o=0.5 besides the aforementioned parameters(λ=1.2, μ=0.20, μ'_{lst}=0.36 and ϕ_d=40°). All these parameters can be determined by a monotonic triaxial compression test(p=98kN/m^2) and a consolidation test.

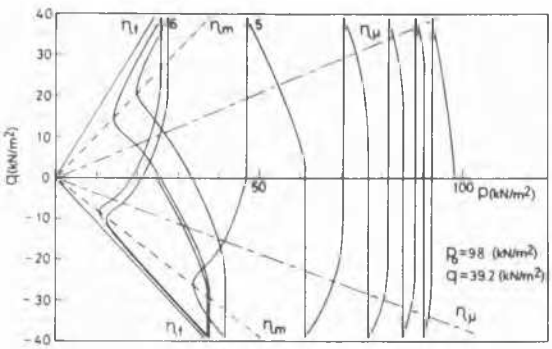

Fig.6 Calculated Effective Stress Path in Undrained Cyclic Triaxial Compression and Extension Test

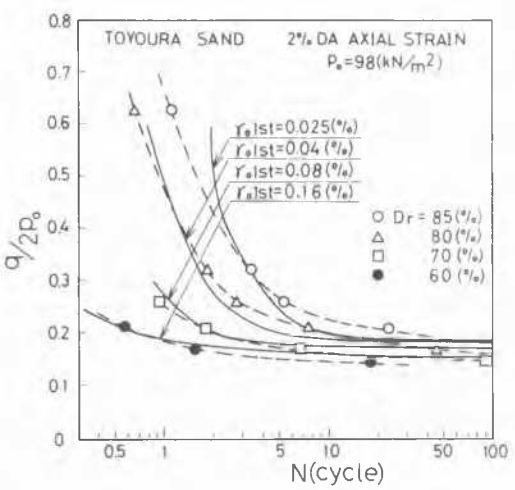

Fig.7 Measured and Calculated Relationships between Cyclic Stress Ratio and Number of Cycles to Produce Initial Liquefaction

CONCLUSIONS

The main results are summarized as follows:
1) A constitutive model for sands was proposed supposing the superposition of strain increments caused by three two-dimensional "mobilized planes" and considering the effect of fabric change under cyclic shear stresses. The results of true triaxial tests along three kinds of rotational stress paths on the octahedral plane were analyzed by the proposed model(see Figs.4 and 5).
2) Adding the strains due to consolidation to the abovementioned model and considering the undrained condition of no volumetric strain increments, the undrained effective stress paths and the liquefaction resistances were calculated(see Figs.6 and 7).

ACKNOWLEDGEMENTS

The authors wish to thank Prof. T. Yamauchi and Prof. T. Nakai at Nagoya Institute of Technology, and Prof. F. Tatsuoka at University of Tokyo for their helpful discussion and support. They are also indebted to Messrs. H. Yamazaki, Y. Matsubara and J. Murai for their experimental assistance.

REFERENCES

Ishihara, K., Tatsuoka, F. and Yasuda, S.(1975). Undrained deformation and liquefaction of sand under cyclic stresses. Soils and Foundations (15), 1, 29-44.

Matsuoka, H.(1974a). A microscopic study on shear mechanism of granular materials. Soils and Foundations (14), 1, 29-43.

Matsuoka, H.(1974b). Stress-strain relationships of sand based on the mobilized plane. Soils and Foundations (14), 2, 47-61.

Matsuoka, H.(1982). Constitutive equation and FE analysis for anisotropic soil. Proc. 4th Int. Conf. on Numerical Methods in Geomechanics, 1, 223-233.

Matsuoka, H. and Geka, H.(1983). A stress-strain model for granular materials considering mechanism of fabric change. Soils and Foundations (23), 2, 83-97.

Matsuoka, H. and Nakai, T.(1974). Stress-deformation and strength characteristics of soil under three different principal stresses. Proc. JSCE, 232, 59-70.

Matsuoka, H. and Nakai, T.(1977). Stress-strain relationship of soil based on the 'SMP'. Proc. Specialty Session 9, 9th ICSMFE, 153-162.

Muramatsu, M.(1981). Undrained cyclic shear behavior of saturated dense sand. Master Thesis, Inst. of Industrial Science, Univ. of Tokyo, Fig.4-9(in Japanese).